

# **DNA-Based Constitutional Dynamic Networks as Functional Modules for Logic Gates and Computing Circuits Operations**

Zhixin Zhou,<sup>a</sup> Jianbang Wang,<sup>a</sup> R. D. Levine,<sup>a</sup> Francoise Remacle<sup>b</sup> and Itamar Willner<sup>a\*</sup>

<sup>a</sup>The Institute of Chemistry, The Hebrew University of Jerusalem, Jerusalem 91904, Israel.

<sup>b</sup>Theoretical Physical Chemistry, UR MolSys B6c, University of Liège, B4000 Liège, Belgium.

E-mail:

[Itamar.willner@mail.huji.ac.il](mailto:Itamar.willner@mail.huji.ac.il)

## Experimental Section

**Materials.** Magnesium chloride were purchased from Sigma-Aldrich. Tris-borate-EDTA (TBE) buffer solution was purchased from Biological Industries Israel BEIT HAEMEK Ltd. (Kibutz Beit-Haemek, Israel). DNA oligonucleotides were purchased from Integrated DNA Technologies Inc. (Coralville, IA). “GelRed nucleic acid gel stain” was purchased from New Biotechnology Ltd.. Ultrapure water from NANOpure Diamond (Barnstead) source was used in all of the experiments.

The oligonucleic acid sequences used in the study include:

**A:** CCATTCAGCGATACGATACAAACTTACACACTTCACAC

**A':** ATCACTATCCACTCTGTTTGTATCGTCACCCATGTTTAGCT

**B:** GTCCTCAGCGATACGATACAAACTACACTACCGTACCA

**B':** ACTCTACTCTATTCTGTTTGTATCGTCACCCATGTTTCAGT

**I<sub>1</sub>:** AGCCTACTCTATTCTTGAAGTGTGTAACGCAGTGGATAGTGAT

**I<sub>2</sub>:** TACGGTAGTGTAGCGTTACACACTTCAAGAATAGAGTAGGCT

**I<sub>3</sub>:** TTCACGTAGACAGCTACTCTATTCTTGTACGGTAGTGTATAGTGGATAG  
TGAT

**I<sub>4</sub>:** TACGGTAGTGTAGCGTTACACACTTCAAGAATAGAGTAGCTGTCTACGT  
GAA

**I<sub>5</sub>:** TACGGTAGTGTACGAGAATAGAGTAGGTTAAGGAGCAACTG

**I<sub>6</sub>:** AGCCTACTCTATTCTTGAAGTGTGTAACGCAGTGGATAGTGAT

**I<sub>7</sub>:** TACGGTAGTGTAGCGTTACACACTTCAAGAATAGAGTAGGCT

**I<sub>8</sub>:** TACGGTAGTGTAAAGAATAGAGTAG

**I<sub>A[+1]</sub>:** GTGTGAAGTGTGTAATGTAAGGAGACTCTG

**I<sub>A[-1]</sub>:** TGGTACGGTAGTGTATGTAAGGAGACTCTG

**I<sub>B[-1]</sub>:** CAGAGTCTCCTTACAAGAATAGAGTAGAGT

**I<sub>B[+1]</sub>:** CAGAGTCTCCTTACAAGAGTGGATAGTGAT

**S<sub>1</sub>:** TTCACGTAGACAGCTACTCTATTCTTGAAGTGTGTAACGCAGTGGATA  
GTGAT

**S<sub>2</sub>:** CAGTTGCTCCTTAACCTACTCTATTCTCGGTGGATAGTGAT

**A-**

**gel:** TCTCTCTCTCTCTCTCTCTCAAGATATCAGCGATACGATACAAACTTAC  
ACACTTCACAC

**A'-**

**gel:** ATCACTATCCACTCTGTTTGTATCGTCACCCATGTTACTCTCTCTCTCT  
CT

**B-gel:** CTGCTCAGCGATACGATACAAACTACACTACCGTACCA

**B'-gel:** ACTCTACTCTATTCTGTTTGTATCGTCACCCATGTTTCGTCA

**Sub1 (AA')**: 5'-FAM-AGCTAATrAGGAATGG-BHQ1-3'

**Sub2 (BB')**: 5'-Cy5-ACTGAATrAGGAGGAC-BHQ2-3'

**Sub3 (BA')**: 5'-FAM-AGCTAATrAGGAGGAC-BHQ1-3'

**Sub4 (AB')**: 5'-ROX-ACTGAATrAGGAATGG-BHQ2-3'

**Sub1-noFQ (AA')**: 5'-AGCTAATrAGGAATGG-3'

**Sub2-noFQ (BB')**: 5'-ACTGAATrAGGAGGAC-3'

**Sub3-noFQ (BA')**: 5'-AGCTAATrAGGAGGAC-3'

**Sub4-noFQ (AB')**: 5'-ACTGAATrAGGAATGG-3'

The ribonucleobase cleavage site, rA, in the substrates of the different Mg<sup>2+</sup>-ion-dependent DNazymes is indicated in bold, the respective Mg<sup>2+</sup>-ion-dependent DNzyme sequences are underlined. All fluorophore/quencher-modified substrates were HPLC-purified. All other strands were not HPLC-purified.

**Measurements.** The excitation of FAM, ROX and Cy5 were performed at 496, 588 and 648, respectively. The emission of FAM, ROX and Cy5 were collected at 516, 608 and 668 at 25 °C, respectively. Fluorescence spectra were recorded with a Cary Eclipse Fluorometer (Varian Inc.). The gels were run on a Hoefer SE 600 electrophoresis unit.

**Preparation of CDN "X".** The CDN "X", composed of the constituents AA', AB', BA' and BB', was prepared as follows. A mixture of A, A', B and B' (2 μM each), in 0.5×TBE buffer (10 mM, pH = 7.2, 20 mM MgCl<sub>2</sub>), was annealed at 65 °C for 5 min, and then cooled down to 25 °C at a rate of 0.33 °C minute<sup>-1</sup>, followed by equilibrating for 1 hour at 25 °C, to yield the mixture of the AA', AB', BA' and BB', the CDN "X". For the reconfiguration of CDN "X" by inputs, the mixture of AA', AB', BA' and BB' (CDN "X", 1 μM), was subjected to the respective inputs (1 μM), and was allowed to equilibrate at 33 °C for a time-interval of 30 min.

#### **Probing the constituents in the CDNs.**

100 μL of the equilibrated mixture of AA', AB', BA' and BB' was treated with the corresponding fluorophore/quencher-modified substrate while the other substrates lacked modification with the fluorophore/quencher pairs. As an example, to probe the content of the constituent AA', 100 μL of the equilibrated mixture of CDN (1 μM) were treated with the substrates: sub1, sub2-noFQ, sub3-noFQ and sub4-noFQ, 5 μL of 100 μM each. Subsequently, the time-dependent fluorescence changes generated by the cleavage of sub1 by the Mg<sup>2+</sup>-ion-dependent DNzyme associated with the AA' were followed at 25 °C. Using the appropriate calibration curves corresponding to the rates of cleavage of the different substrates by different concentrations of the intact constituents, the contents of the constituents in the different CDNs were evaluated. It should be noted that for probing the operation of the CDNs, we examine

the output generated by each of the constituents by using one fluorophore/quencher-modified substrate for the target constituent, while all other substrates are non-labeled. This approach is due to cost-effectiveness associated with the analytical procedures to characterize the system. In principle, one may apply four different fluorophore/quencher functionalized substrates to measure simultaneously the response of all reporter units.

To prove, however, the capacity to follow simultaneously the outputs of a CDN module by a composition of four different fluorophore/quencher-modified substrates we, present in Figure S29. The output simultaneous output results of the logic gate presented in Figure 1. In this case, we use the following substrates:

**Sub1** (AA'): 5'- FAM-AGCTAATrAGGAATGG-BHQ1-3'

**Sub2** (BB'): 5'-Cy5-ACTGAATrAGGAGGAC-BHQ2-3'

**Sub3** (BA'): 5'-Cy5.5-AGCTAATrAGGAGGAC-BHQ1-3'

**Sub4** (AB'): 5'-ROX-ACTGAATrAGGAATGG-BHQ2-3'

(Note here we exchanged one of the two FAM-modified substrates with the expensive Cy5.5-functionalized substrate) Figure S29 shows the time-dependent fluorescence changes of the reporter units associated with CDN module X, Figure 1A upon subjecting the CDN X to input  $I_1$ . The resulting output signals overlay with the results presented using the individual substrate to assay to computational module.

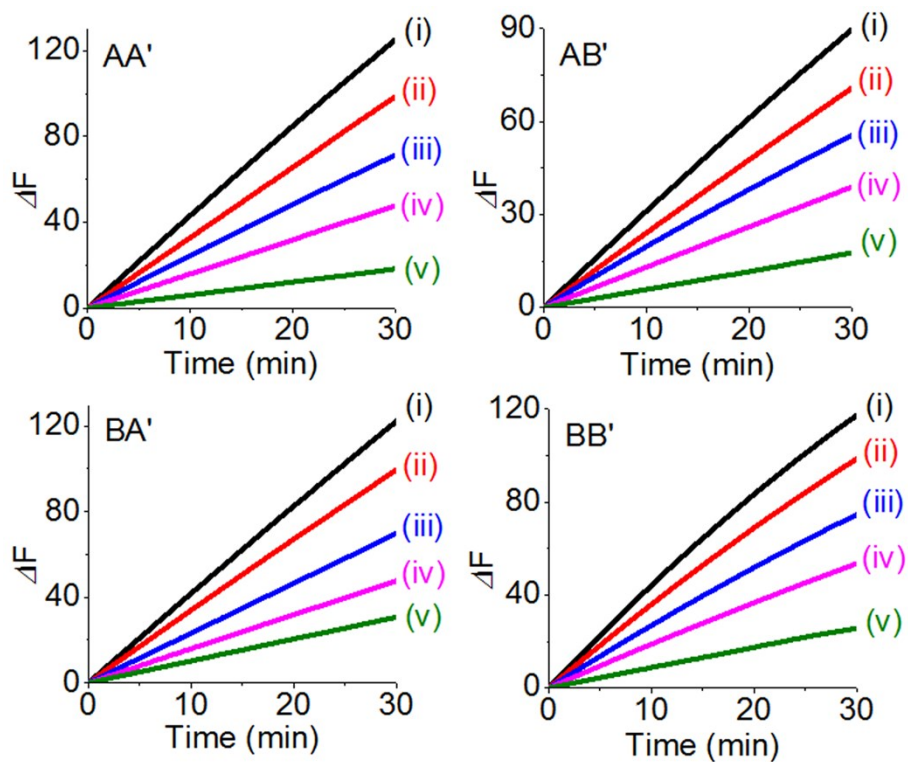


**Figure S1.** Time-dependent fluorescence changes generated upon the cleavage of the fluorophore/quencher-modified substrates by the respective Mg<sup>2+</sup>-ion-DNAzyme reporter units associated with the individual intact constituents at variable concentrations: (i) 1  $\mu\text{M}$ , (ii) 0.8  $\mu\text{M}$ , (iii) 0.6  $\mu\text{M}$ , (iv) 0.4  $\mu\text{M}$ , and (v) 0.2  $\mu\text{M}$ .

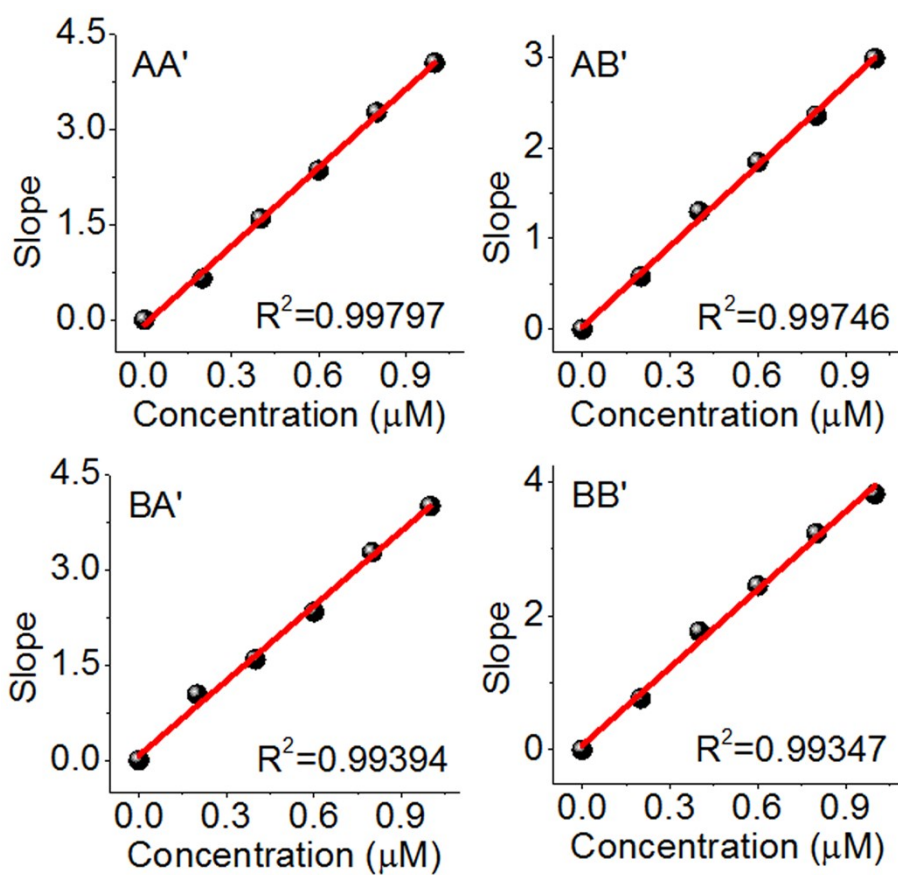


**Figure S2.** Corresponding calibration curves of the catalytic rates of the different constituents as a function of their concentrations, derived from the data shown in Figure S1.

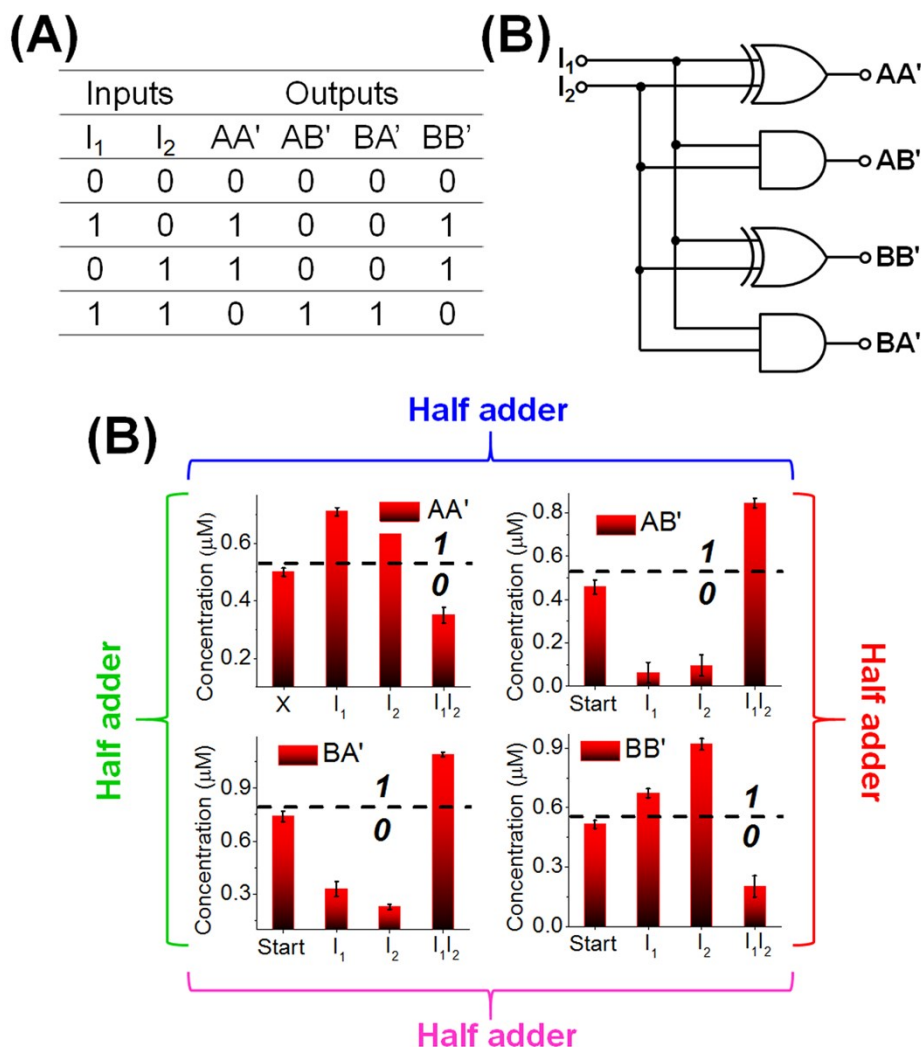


**Figure S3.** (A) Truth-Table of the CDN half-adder driven by  $I_1$  and  $I_2$  as inputs and the reporter units associated with constituents  $AA'$ ,  $AB'$ ,  $BA'$  and  $BB'$  as outputs. (B) Scheme of the logic gate driven by the CDN in the presence of  $I_1$  and  $I_2$ . (C) Content changes generated by the reporter units associated with constituents  $AA'$ ,  $AB'$ ,  $BA'$  and  $BB'$  acting as outputs in the form of a bar presentation, demonstrating the operation of the CDN “X” as functional unit activating four different logically equivalent output signals of a single half adder using  $I_1$  and  $I_2$  as inputs.

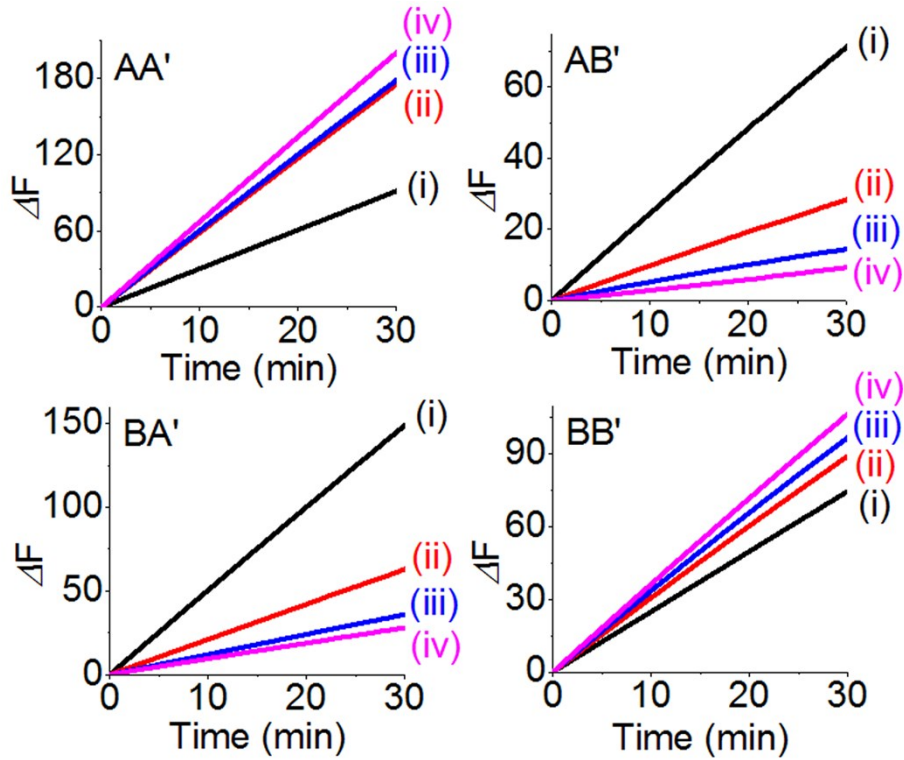


**Figure S4.** Time-dependent fluorescence changes generated by the reporter units associated with the constituents of CDN "X", in the presence of variable concentrations of  $I_1$ : (i)  $0 \mu\text{M}$ , (ii)  $0.8 \mu\text{M}$ , (iii)  $1.0 \mu\text{M}$ , (iv)  $1.2 \mu\text{M}$ .

We were questioned by one of the reviewers regarding the effects of concentration changes of the input on the sensitivity of the output signal and possible "errors" generated by the computational modules. To address this issue, we examined, as example, the effect of concentration changes of input  $I_1$  on the computational module presented in Figures 1 and 2.

Figure S4 presents the time-dependent fluorescence changes of the reporter units associated with the constituents AA', AB', BA', and BB' of CDN "X", upon altering the concentrations of the input  $I_1$  in the range  $0.8 \mu\text{M} - 1.2 \mu\text{M}$  (the concentrations of  $I_1$  in the experiment reported in Figure 2 corresponded to  $1 \mu\text{M}$ ). The results demonstrate that error deviations corresponding to  $\pm 20\%$  of input concentration provided reliable difference in the output signals.

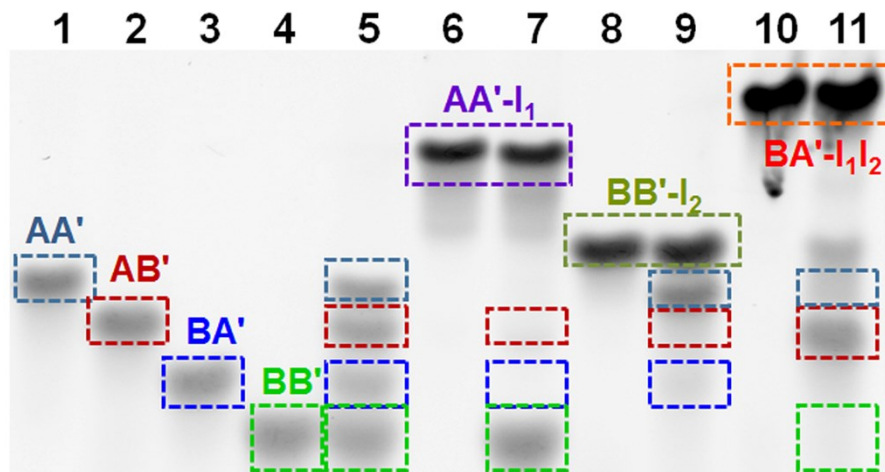


**Figure S5.** Electrophoretic image of the separated bands generated upon  $I_1/I_2$ -driven reconfiguration of CDN “X” that yields in parallel the four outputs shown in Figure 1 of the main text. For comparison, the separated intact constituents AA’ (lane 1), AB’ (lane 2), BA’ (lane 3), BB’ (lane 4), AA’- $I_1$  (lane 6), BB’- $I_2$  (lane 8) and BA’- $I_1I_2$  (lane 10). Lane 5: the separated bands of CDN “X”. Lane 7: the separated bands of  $I_1$ -induced reconfiguration of CDN “X”; Lane 9: the separated bands of  $I_2$ -induced reconfiguration of CDN “X”; Lane 11: the separated bands of  $I_1I_2$ -induced reconfiguration of CDN “X”. It should be noted that the constituents, AA’, BB’, AB’, and BA’ used in the fluorescent evaluation of the contents of the CDN constituents have almost identical base lengths, and these are non-separable by electrophoretic separations. To support the fluorescent results by electrophoretic separations, we extended the length of the components A and A’ by innocent tethers (that do not affect the equilibrated compositions) as outlined in the description of the strands (supporting information). This approach allowed us to generate the separate bands, outlined in Figure S5.

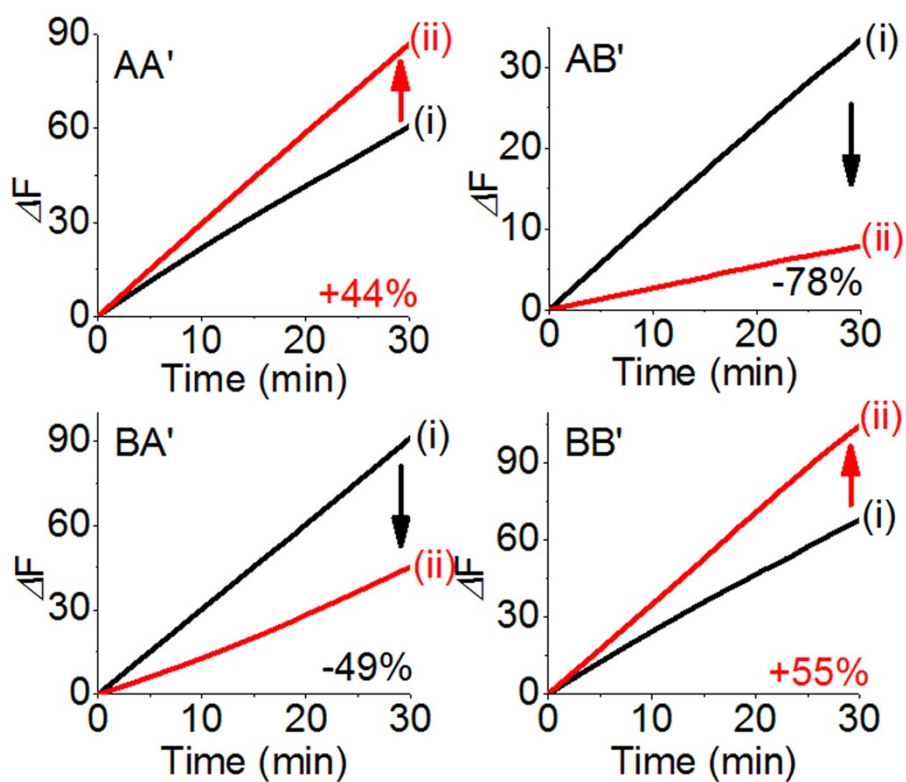


**Figure S6.** Time-dependent fluorescence changes generated by the reporter units associated with the constituents of CDN “X”: Before subjecting to selector  $S_1$  (i) and after treatment with selector  $S_1$  (ii).

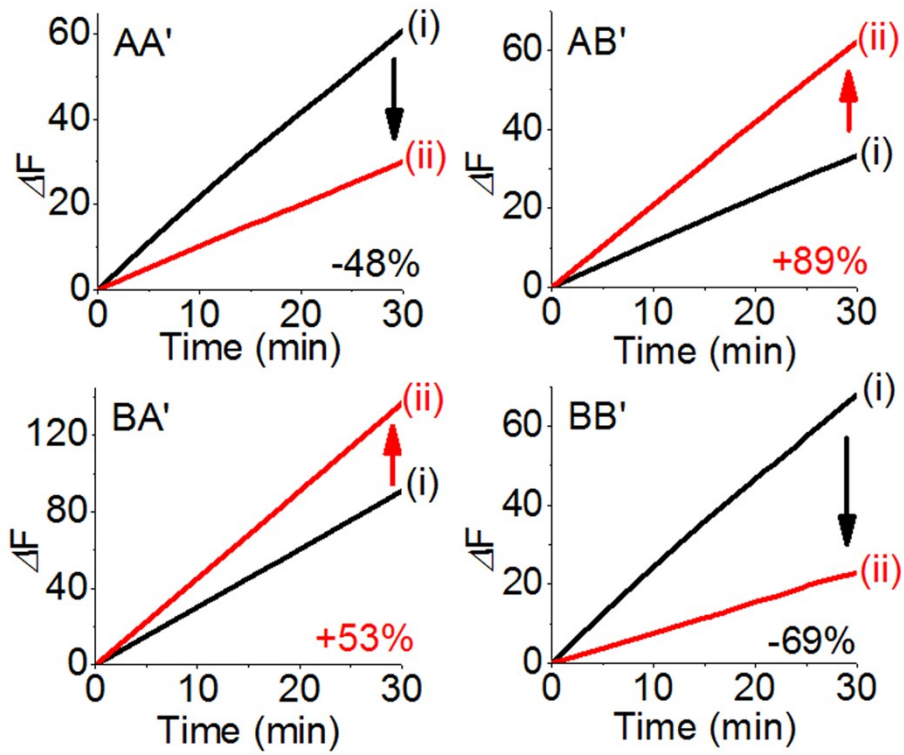


**Figure S7.** Time-dependent fluorescence changes generated by the reporter units associated with the constituents of CDN “X”: Before subjecting to input  $I_3$  (i) and after treatment with input  $I_3$  (ii).

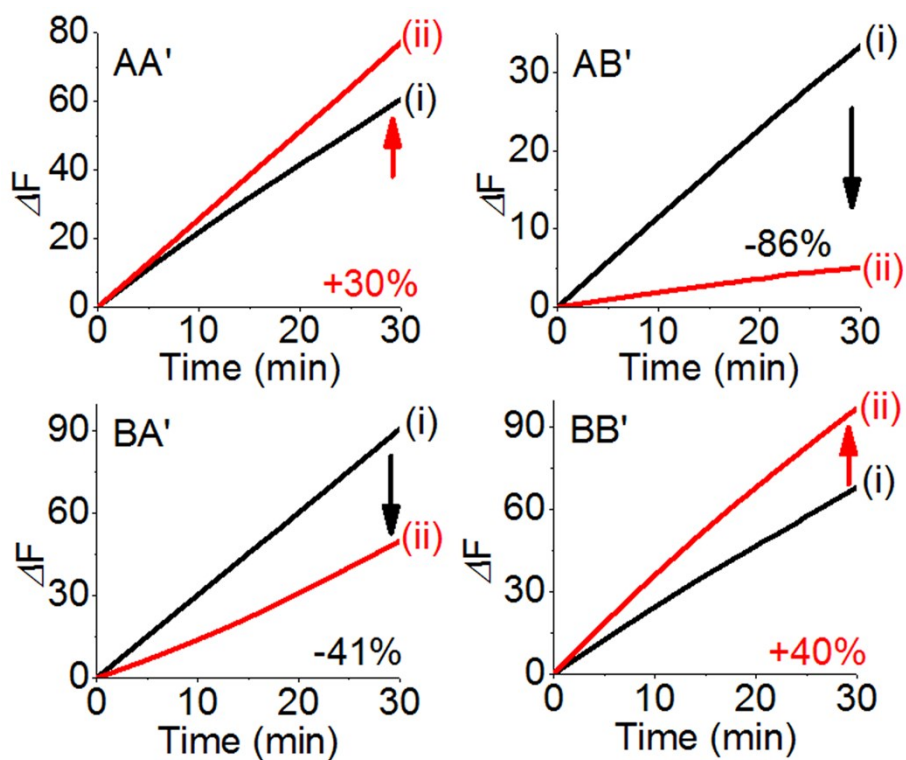


**Figure S8.** Time-dependent fluorescence changes generated by the reporter units associated with the constituents of CDN “X”: Before subjecting to input  $I_4$  (i) and after treatment with input  $I_4$  (ii).

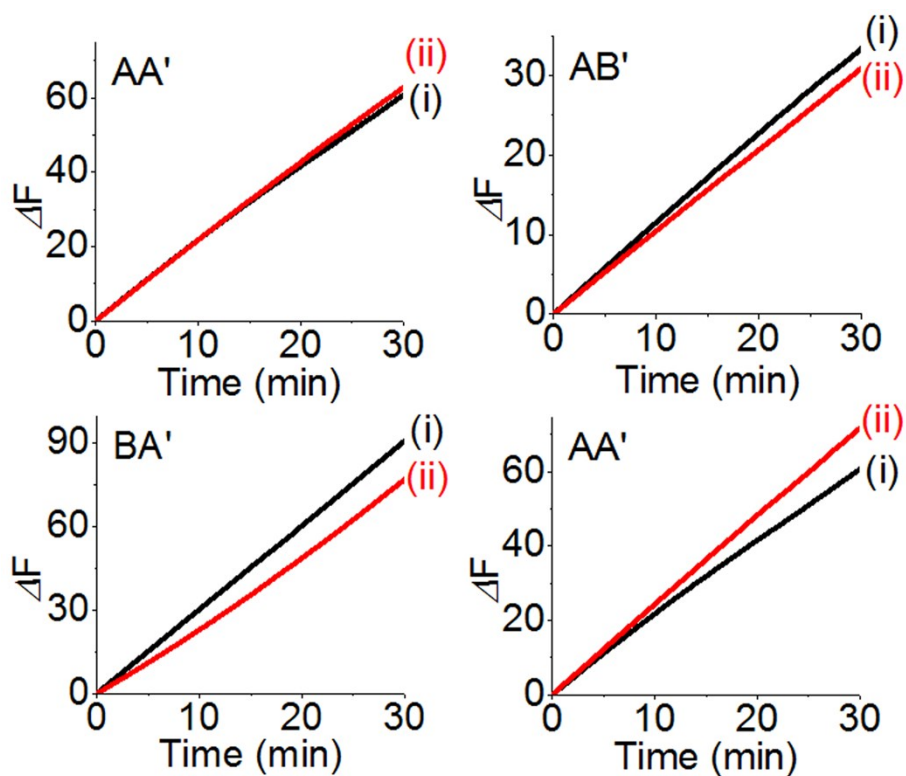


**Figure S9.** Time-dependent fluorescence changes generated by the reporter units associated with the constituents of CDN “X”: Before subjecting to selector/input  $S_1I_3$  (i) and after treatment with selector/input  $S_1I_3$  (ii).

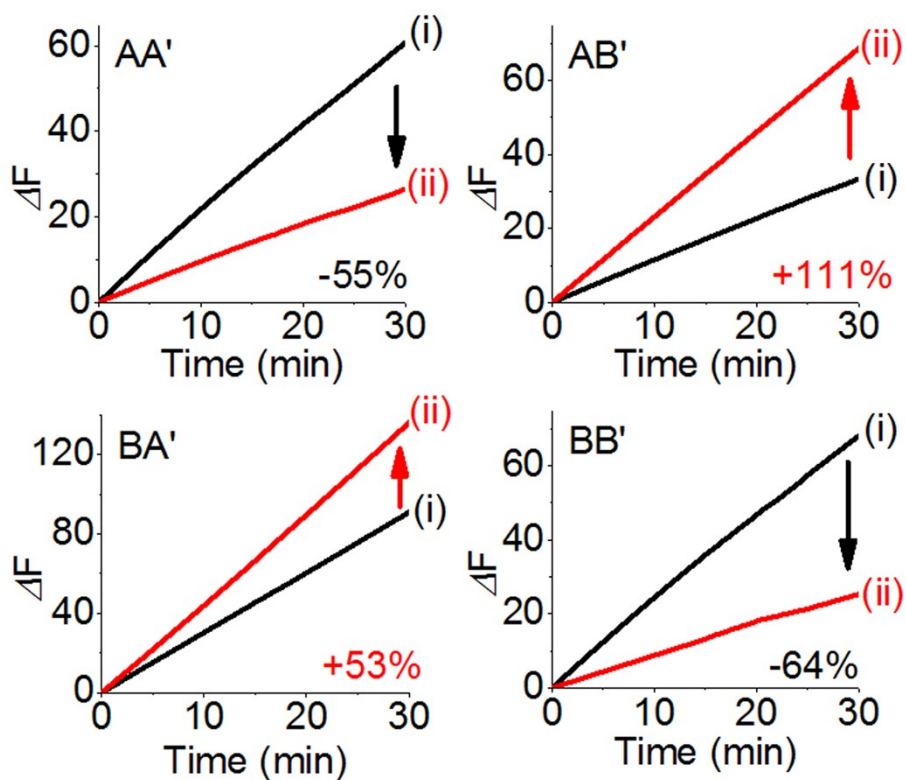


**Figure S10.** Time-dependent fluorescence changes generated by the reporter units associated with the constituents of CDN “X”: Before subjecting to selector/input  $S_1I_4$  (i) and after treatment with selector/input  $S_1I_4$  (ii).

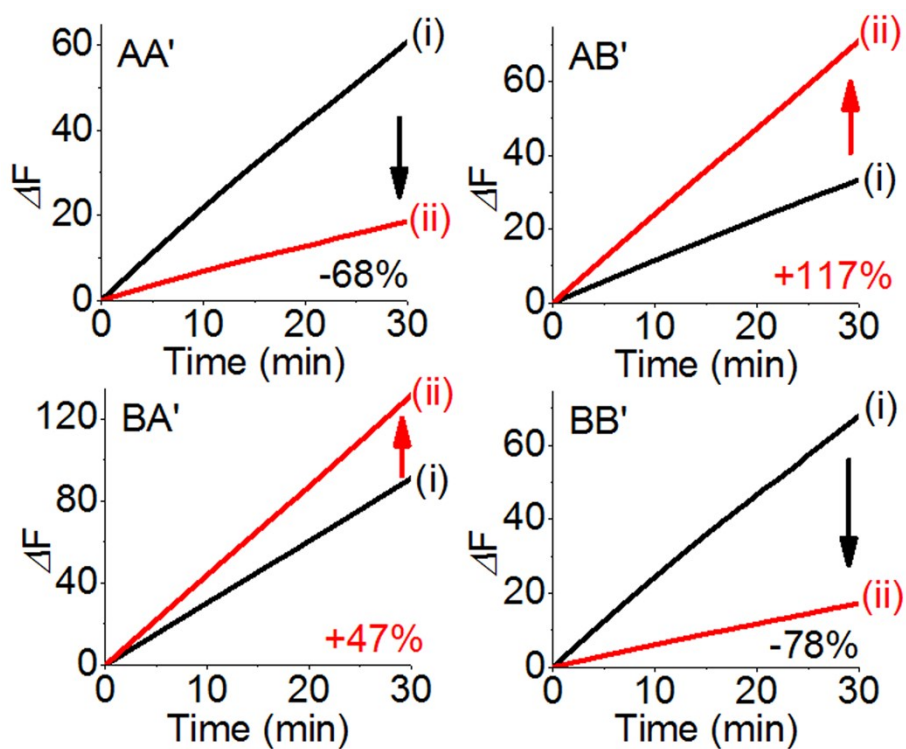


**Figure S11.** Time-dependent fluorescence changes generated by the reporter units associated with the constituents of CDN “X”: Before subjecting to inputs  $I_3I_4$  (i) and after treatment with inputs  $I_3I_4$  (ii).

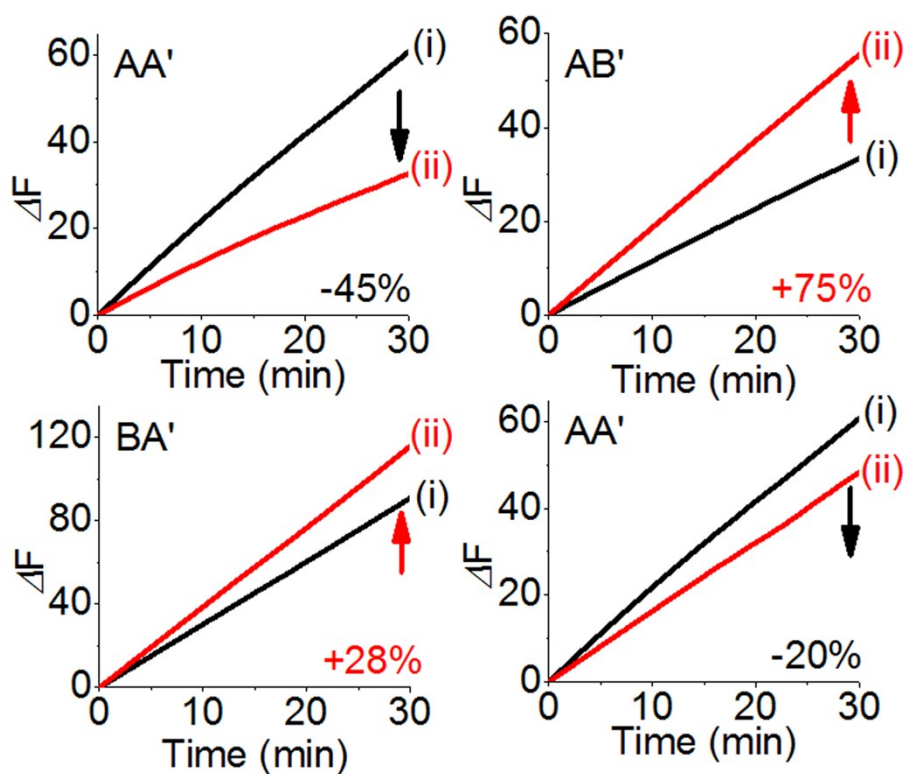


**Figure S12.** Time-dependent fluorescence changes generated by the reporter units associated with the constituents of CDN “X”: Before subjecting to selector/inputs  $S_1I_3I_4$  (i) and after treatment with selector/inputs  $S_1I_3I_4$  (ii).

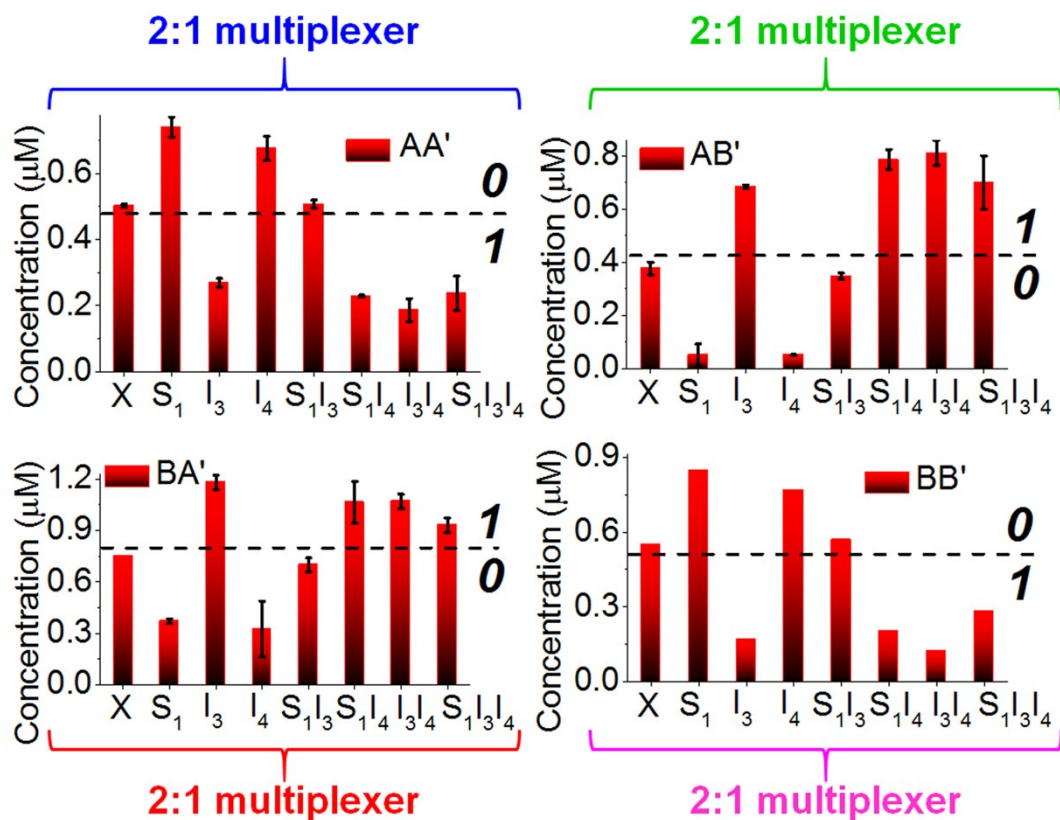


**Figure S13.** Content changes generated by the reporter units associated with constituents AA', AB', BA' and BB' acting as outputs in the form of a bar presentation, demonstrating the operation of the CDN "X" as functional unit activating four logically redundant output signals of a single 2:1 multiplexer logic gates using S<sub>1</sub> as selector and I<sub>3</sub> and I<sub>4</sub> as inputs.

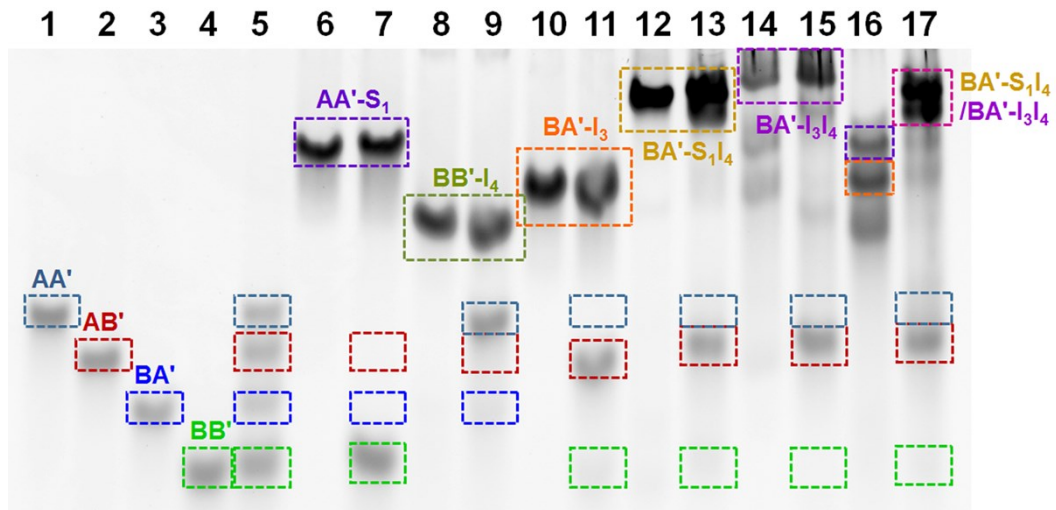


**Figure S14.** Electrophoretic image of the separated bands generated upon inputs/selector-driven reconfiguration of CDN “X” that yields the 2:1 multiplexer displayed in Figure 4. For comparison, the separated intact constituents AA’ (lane 1), AB’ (lane 2), BA’ (lane 3), BB’ (lane 4), AA’-S<sub>1</sub> (lane 6), BB’-I<sub>4</sub> (lane 8), BA’-I<sub>3</sub> (lane 10), BA’-S<sub>1</sub>I<sub>4</sub> (lane 12) and BA’-I<sub>3</sub>I<sub>4</sub> (lane 14). Lane 5: the separated bands of CDN “X”. Lane 7: the separated bands of S<sub>1</sub>-induced reconfiguration of CDN “X”. Lane 9: the separated bands of I<sub>4</sub>-induced reconfiguration of CDN “X”. Lane 11: the separated bands of I<sub>3</sub>-induced reconfiguration of CDN “X”. Lane 13: the separated bands of S<sub>1</sub>I<sub>4</sub>-induced reconfiguration of CDN “X”. Lane 15: I<sub>3</sub>I<sub>4</sub>-induced reconfiguration of CDN “X”. Lane 16: the separated bands of S<sub>1</sub>I<sub>3</sub>-induced reconfiguration of CDN “X”. Lane 17: the separated bands of S<sub>1</sub>I<sub>3</sub>I<sub>4</sub>-induced reconfiguration of CDN “X”.

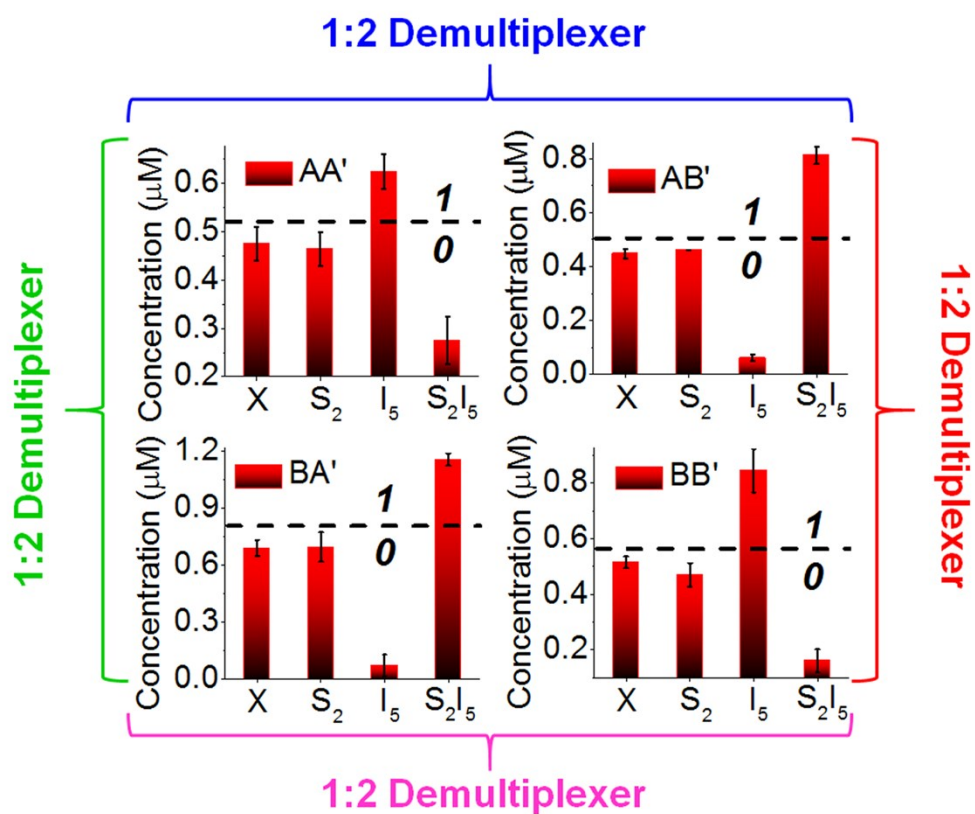


**Figure S15.** Content changes generated by the reporter units associated with constituents AA', AB', BA' and BB' acting as outputs in the form of a bar presentation, demonstrating the operation of the CDN "X" as functional unit activating four logically equivalent pairs of output signals of a single 1:2 demultiplexer using I<sub>5</sub> as input and S<sub>2</sub> as selector.

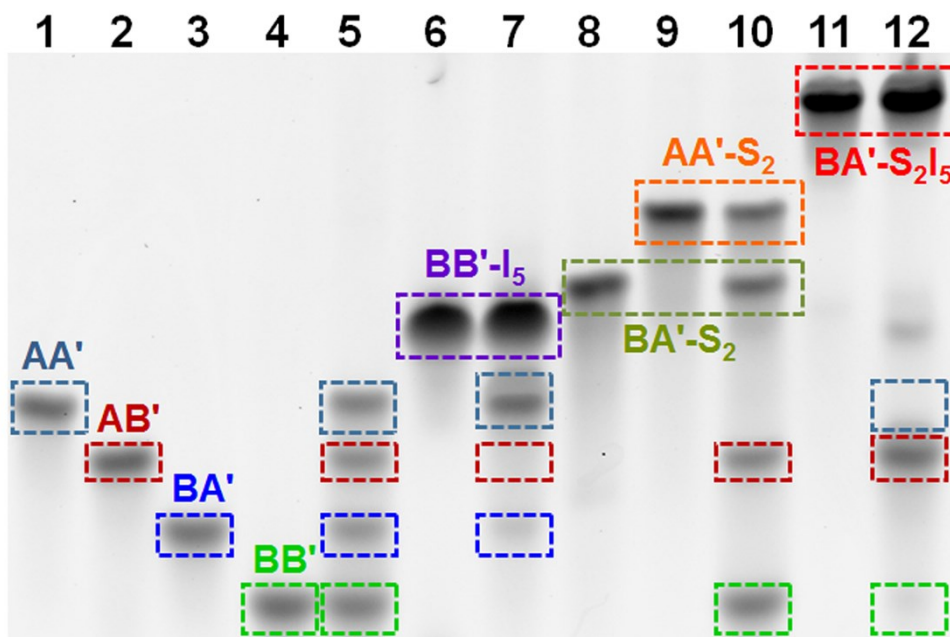


**Figure S16.** Electrophoretic image of the separated bands generated upon S<sub>2</sub>/I<sub>5</sub>-driven reconfiguration of CDN "X" that yields demultiplexer displayed in Figure 5. For comparison, the separated intact constituents AA' (lane 1), AB' (lane 2), BA' (lane 3), BB' (lane 4), BB'-I<sub>5</sub> (lane 6), BA'-S<sub>2</sub> (lane 8), AA'-S<sub>2</sub> (lane 9) and BA'-S<sub>2</sub>I<sub>5</sub> (lane 11). Lane 5: the separated bands of CDN "X". Lane 7: the separated bands of I<sub>5</sub>-induced reconfiguration of CDN "X". Lane 10; the separated bands of S<sub>2</sub>-induced reconfiguration of CDN "X". Lane 12: the separated bands of S<sub>2</sub>I<sub>5</sub>-induced reconfiguration of CDN "X".

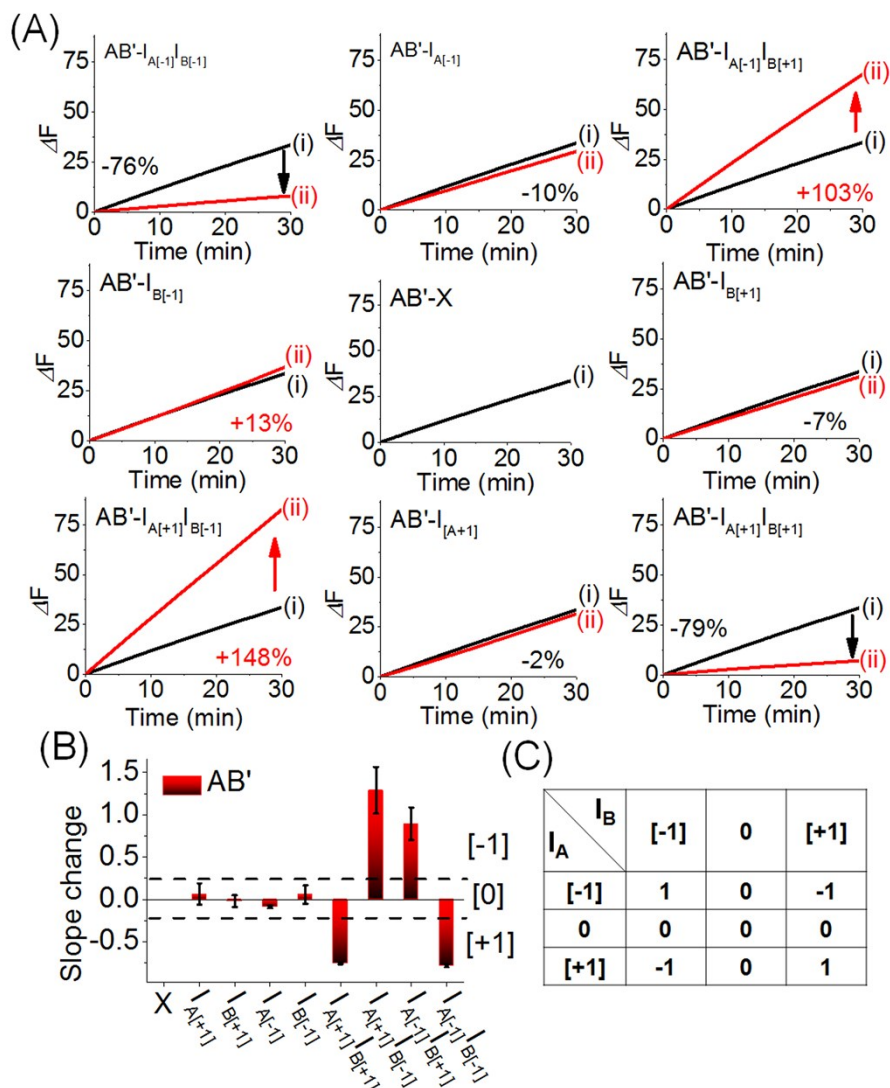


**Figure S17.** (A) Time-dependent fluorescence changes generated by the reporter unit associated with AB' upon subjecting CDN to the different inputs outlined in Figure 8. Curves (i) correspond to the response of the AB' reporter unit before the application of any inputs, curves ii correspond to the results of applying different inputs. (B) Bar presentation of the fluorescence changes associated with the constituent AB' in the presence of the different inputs. (C) Truth-table corresponding to the ternary  $3 \times 3$  multiplication matrix generated by AB'.

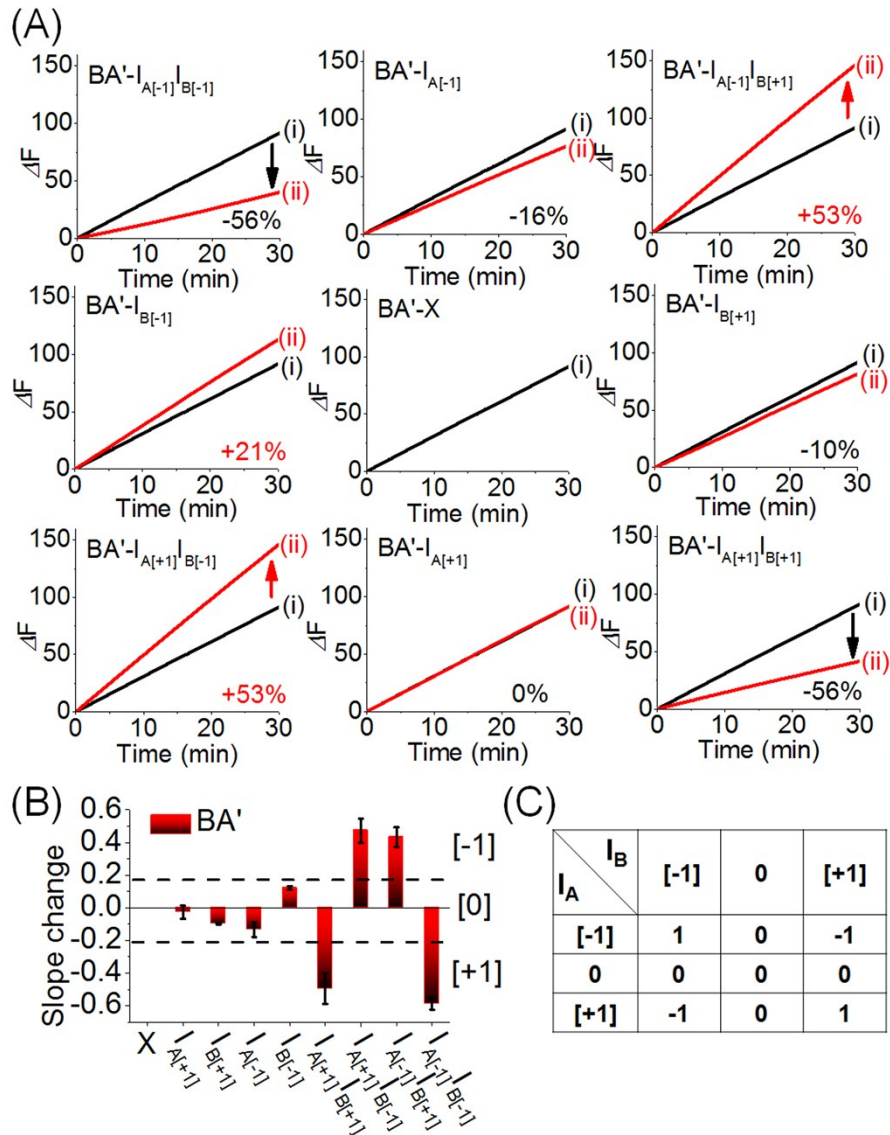


**Figure S18.** (A) Time-dependent fluorescence changes generated by the reporter unit associated with BA' upon subjecting CDN to the different inputs outlined in Figure 8. Curves (i) correspond to the response of the BA' reporter unit before the application of any inputs, curves ii correspond to the results of applying different inputs. (B) Bar presentation of the fluorescence changes associated with the constituent BA' in the presence of the different inputs. (C) Truth-table corresponding to the ternary  $3 \times 3$  multiplication matrix generated by BA'.

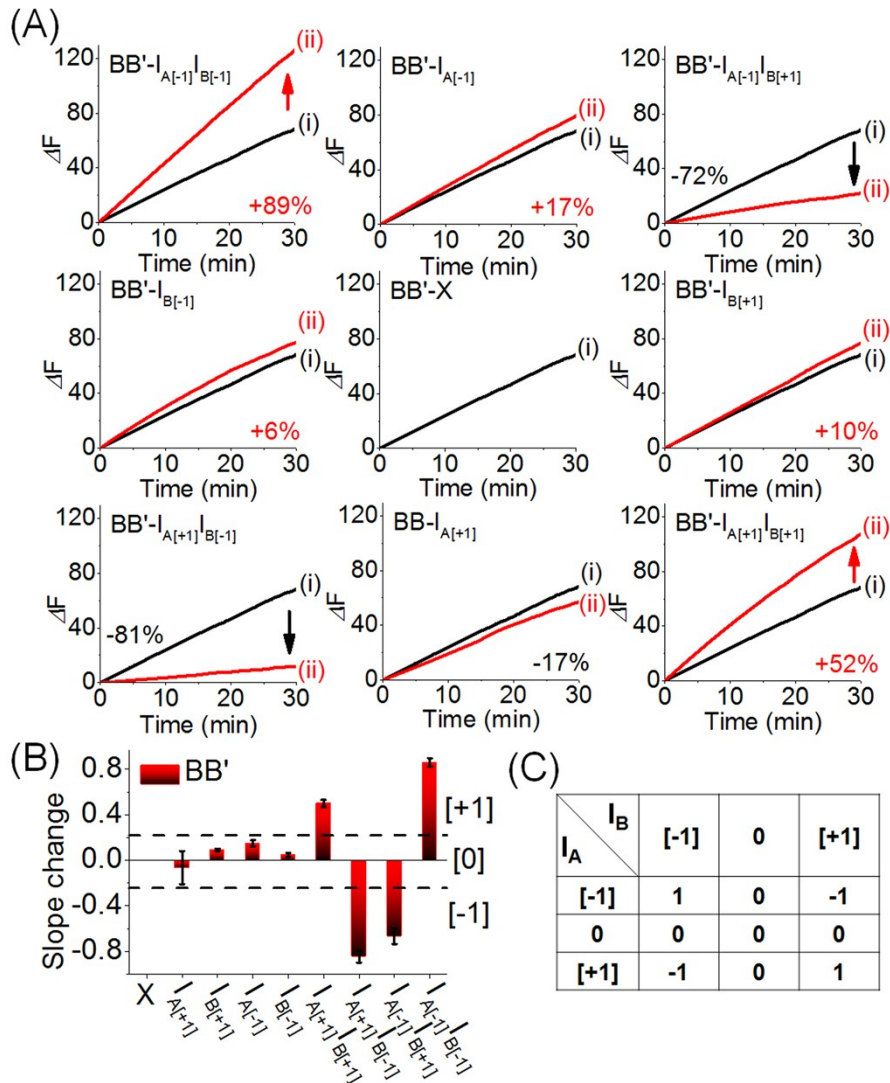


**Figure S19.** (A) Time-dependent fluorescence changes generated by the reporter unit associated with BB' upon subjecting CDN to the different inputs outlined in Figure 8. Curves (i) correspond to the response of the BB' reporter unit before the application of any inputs, curves ii correspond to the results of applying different inputs. (B) Bar presentation of the fluorescence changes associated with the constituent BB' in the presence of the different inputs. (C) Truth-table corresponding to the ternary 3x3 multiplication matrix generated by BB'.

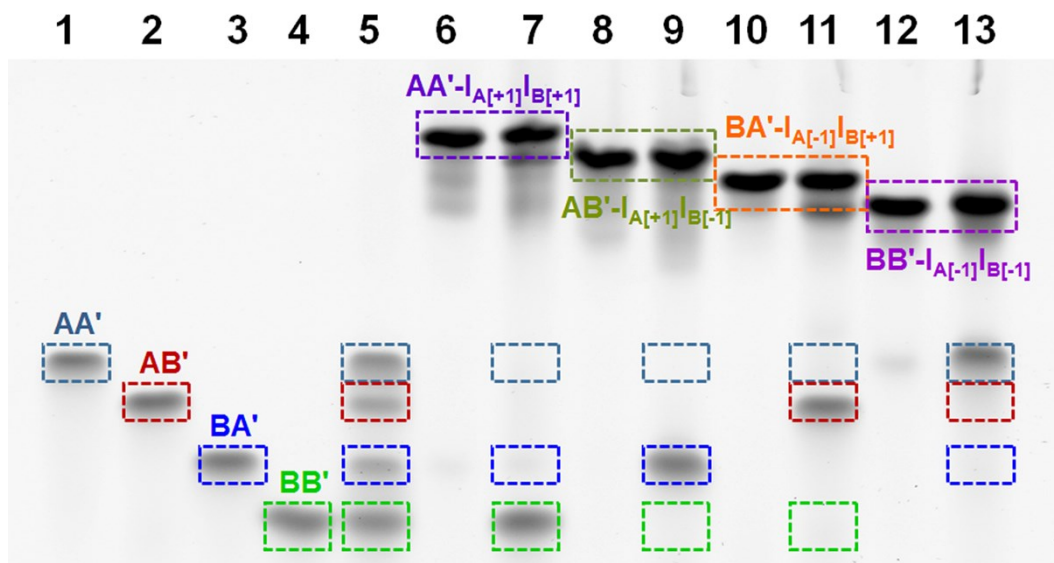


**Figure S20.** Electrophoretic image of the separated bands generated upon  $I_{A[+1]}/I_{B[+1]}/I_{A[-1]}/I_{B[-1]}$ -driven reconfiguration of CDN “X” that yields the multiplication matrix displayed in Figure 8. For comparison, the separated intact constituents AA’ (lane 1), AB’ (lane 2), BA’ (lane 3), BB’ (lane 4), AA’- $I_{A[+1]}I_{B[+1]}$  (lane 6), AB’- $I_{A[+1]}I_{B[-1]}$  (lane 8), BA’- $I_{A[-1]}I_{B[+1]}$  (lane 10) and BB’- $I_{A[-1]}I_{B[-1]}$  (lane 12). Lane 5- CDN “X”; lane 7- $I_{A[+1]}I_{B[+1]}$ -induced reconfiguration of CDN “X”; lane 9- $I_{A[+1]}I_{B[-1]}$ -induced reconfiguration of CDN “X”; lane 11- $I_{A[-1]}I_{B[+1]}$ -induced reconfiguration of CDN “X”; lane 13- $I_{A[-1]}I_{B[-1]}$ -induced reconfiguration of CDN “X”.

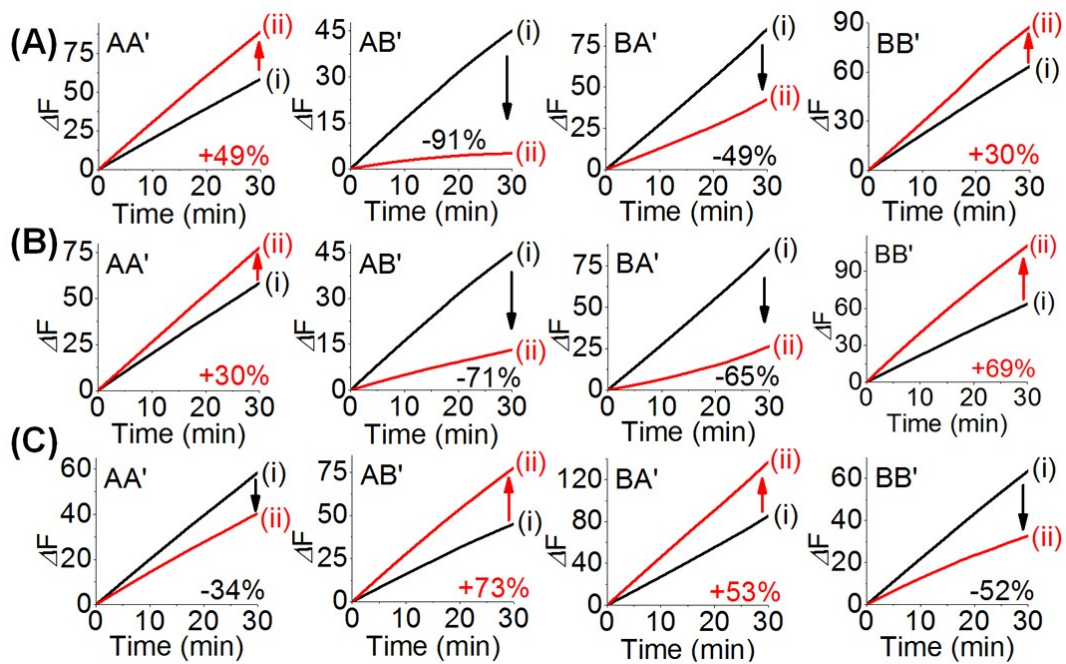


**Figure S21.** Time-dependent fluorescence changes generated by the reporter units associated with the constituents of CDN “X”: (A) Before subjecting to input  $I_6$  (i) and after treatment with input  $I_6$  (ii); (B) Before subjecting to input  $I_7$  (i) and after treatment with input  $I_7$  (ii); (C) Before subjecting to inputs  $I_6I_7$  (i) and after treatment with inputs  $I_6I_7$  (ii). It should be noted that Figure S21 and Figure 2 are the same because the sequence of  $I_1I_2$  and  $I_6I_7$  are the same.

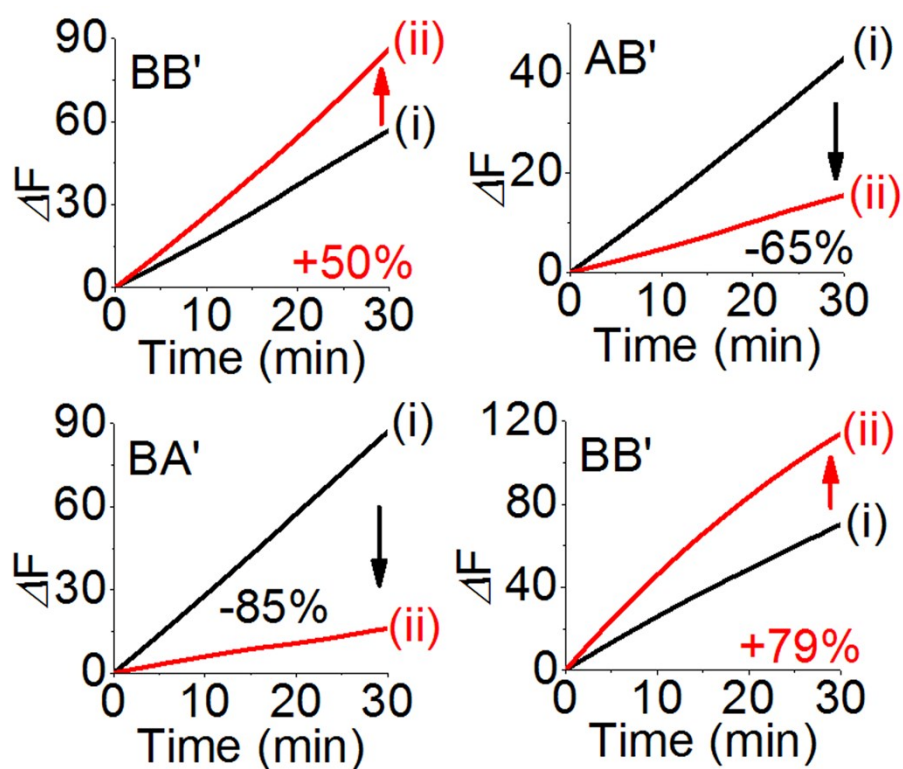


**Figure S22.** Time-dependent fluorescence changes generated by the reporter units associated with the constituents of CDN "X": Before subjecting to input  $I_8$  (i) and after treatment with input  $I_8$  (ii).

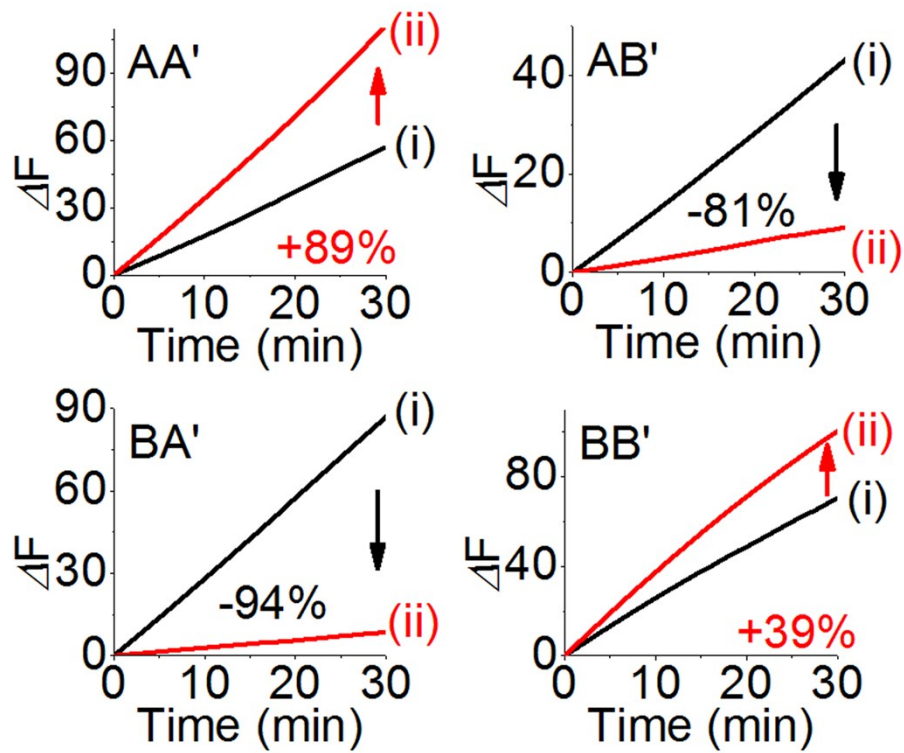


**Figure S23.** Time-dependent fluorescence changes generated by the reporter units associated with the constituents of CDN “X”: Before subjecting to inputs  $I_6I_8$  (i) and after treatment with inputs  $I_6I_8$  (ii).

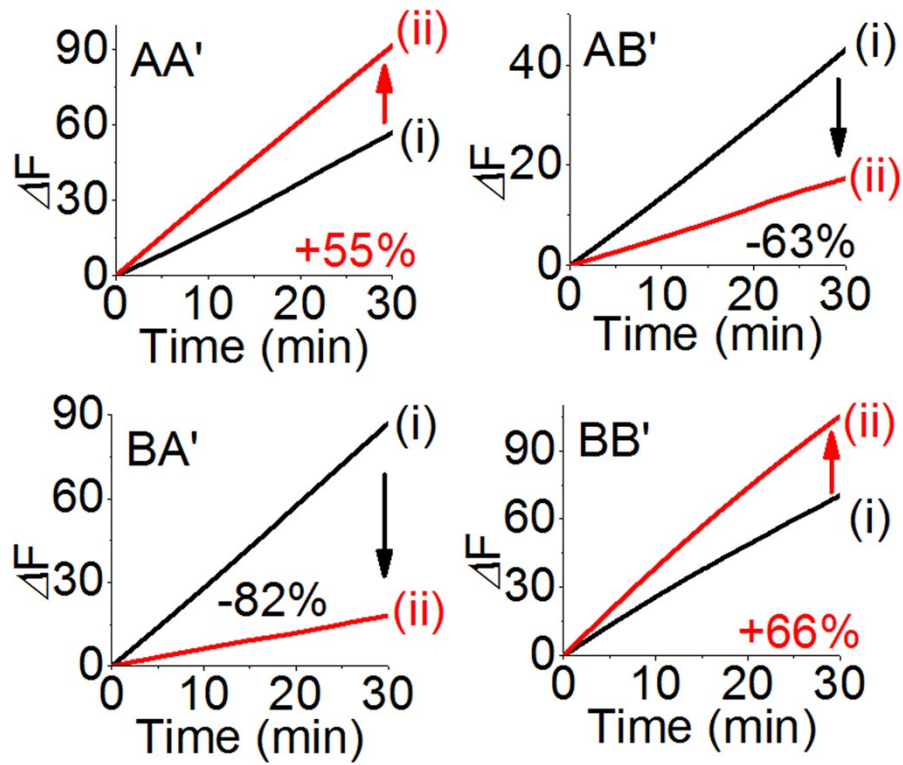


**Figure S24.** Time-dependent fluorescence changes generated by the reporter units associated with the constituents of CDN “X”: Before subjecting to inputs  $I_7I_8$  (i) and after treatment with inputs  $I_7I_8$  (ii).

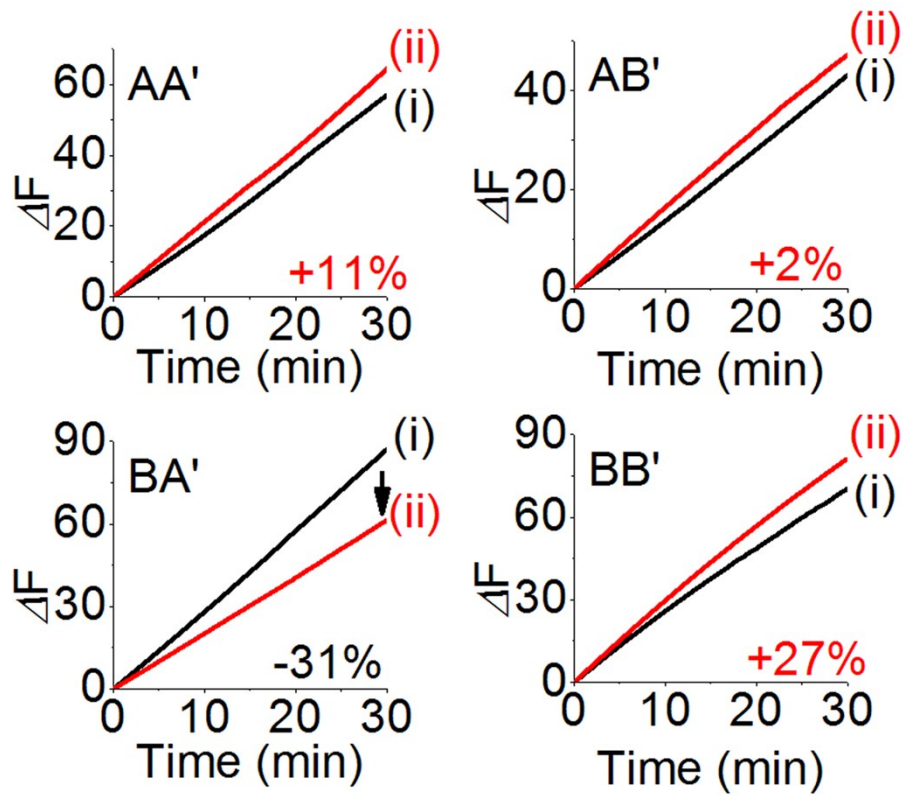


**Figure S25.** Time-dependent fluorescence changes generated by the reporter units associated with the constituents of CDN “X”: Before subjecting to inputs  $I_6I_7I_8$  (i) and after treatment with inputs  $I_6I_7I_8$  (ii).

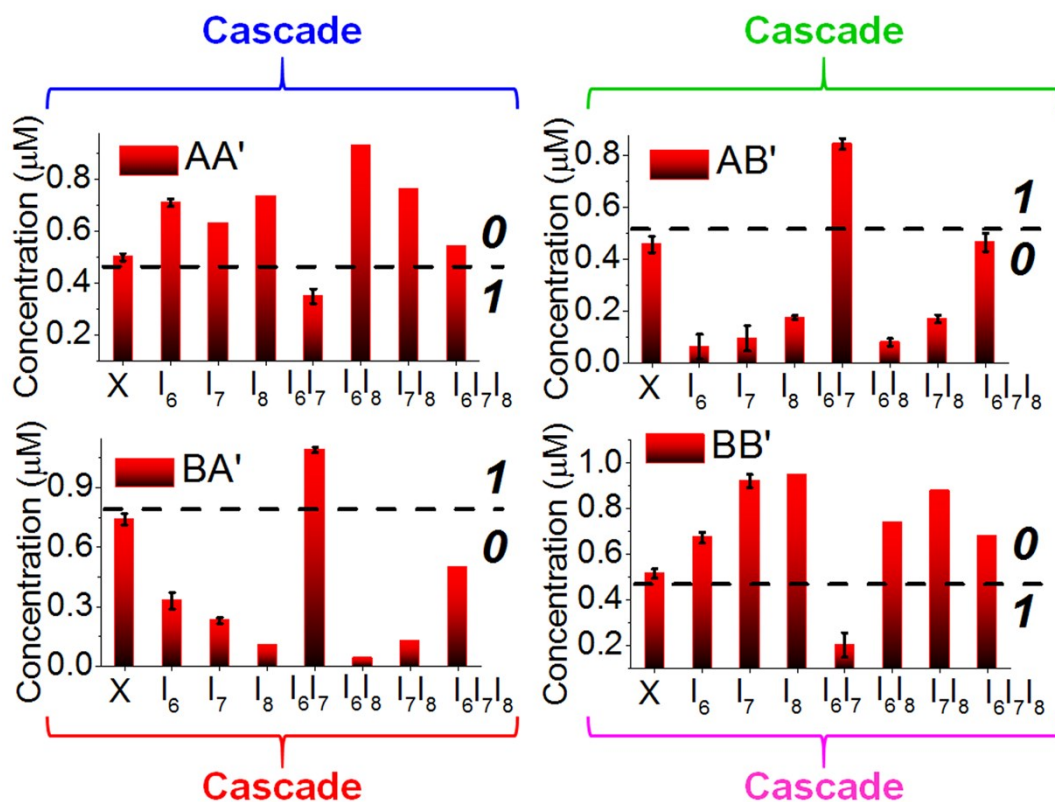


**Figure S26.** Content changes generated by the reporter units associated with constituents AA', AB', BA' and BB' acting as outputs in the form of a bar presentation, demonstrating the operation of the CDN "X" as functional unit activating four different output signals of a single AND-InhibAND cascade using I<sub>6</sub>, I<sub>7</sub> and I<sub>8</sub> as inputs.

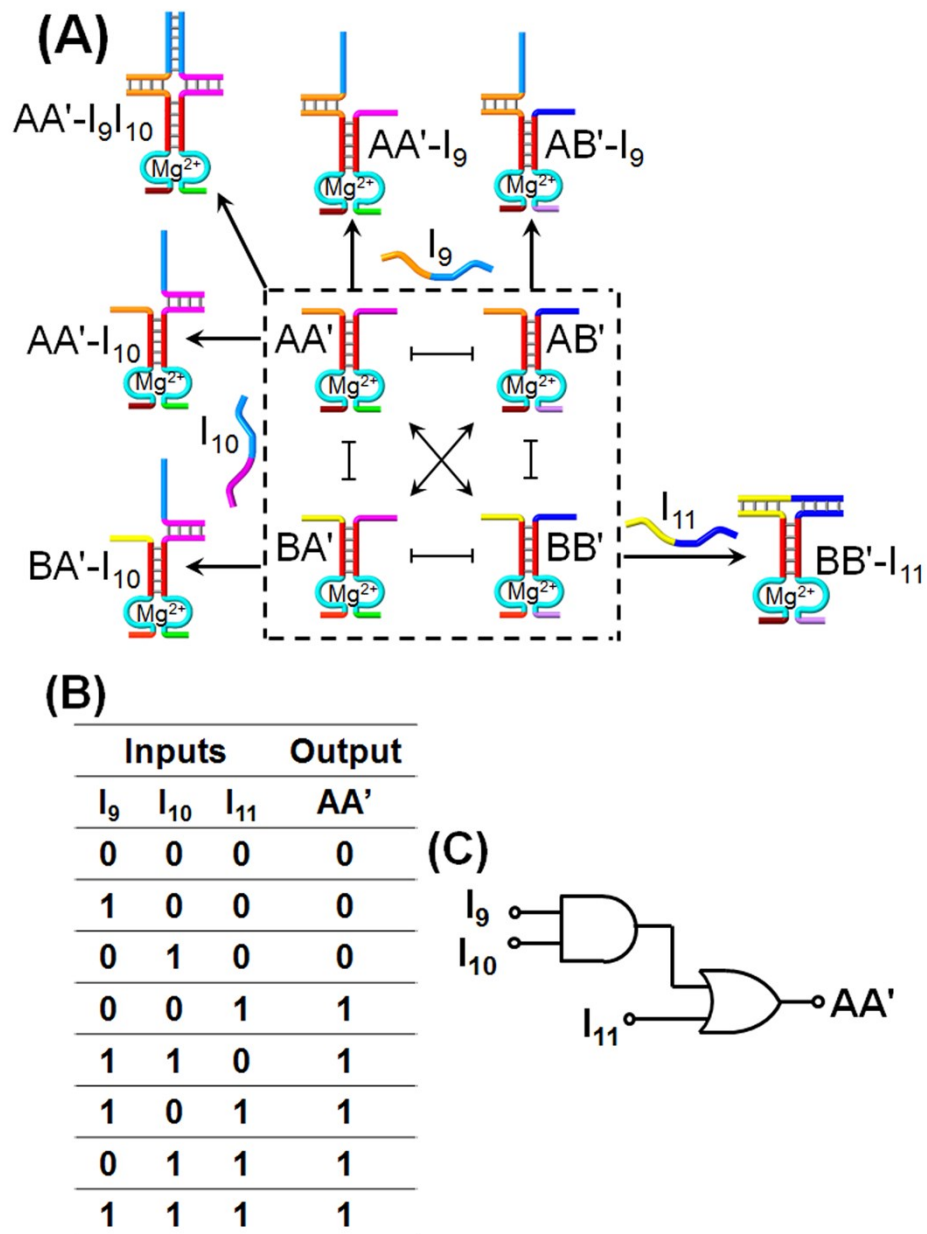


**Figure S27.** Schematic CDN-guided operation of AND–OR cascade circuit. (B) Truth-Table corresponding to the CDN AND–OR cascade driven by the inputs  $I_9$ ,  $I_{10}$  and  $I_{11}$  using the content changes generated by the DNAzyme reporter unit associated with  $AA'$  as output. (C) Scheme of the AND–OR cascade operation driven by the inputs and transduced by the constituent  $AA'$  as output.

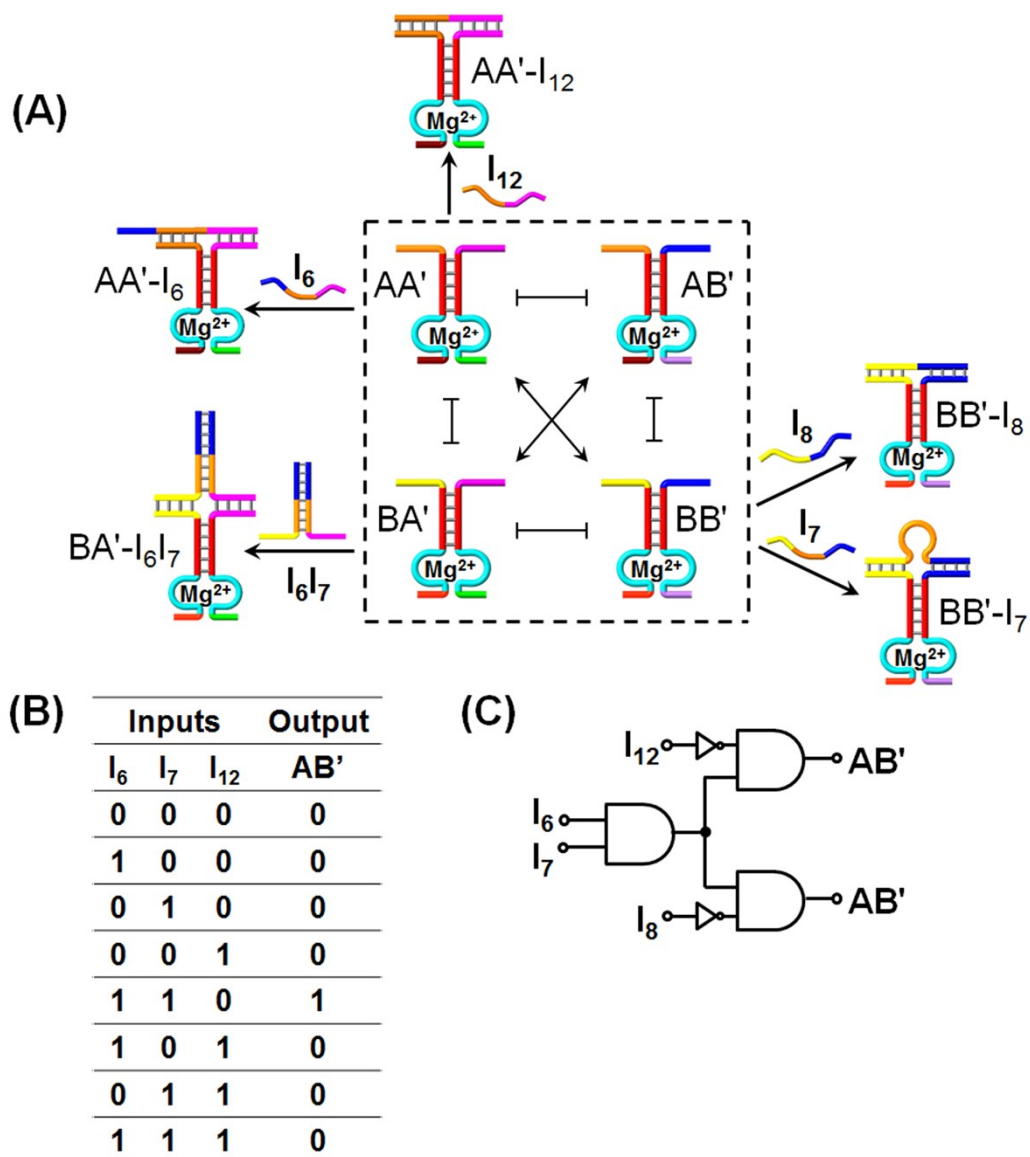


**Figure S28.** Schematic CDN-guided operation of fan-out circuit where the output of an AND gate is directed to two downstream InhibitAND gates. (B) Truth-table corresponding to the CDN AND–InhibitAND cascade driven by the inputs  $I_6$ ,  $I_7$  and  $I_{12}$  using the content changes generated by the DNazyme reporter unit associated with  $AB'$  as output. (C) Scheme of the fan-out circuits driven by the inputs and transduced by the constituent  $AB'$  as output.

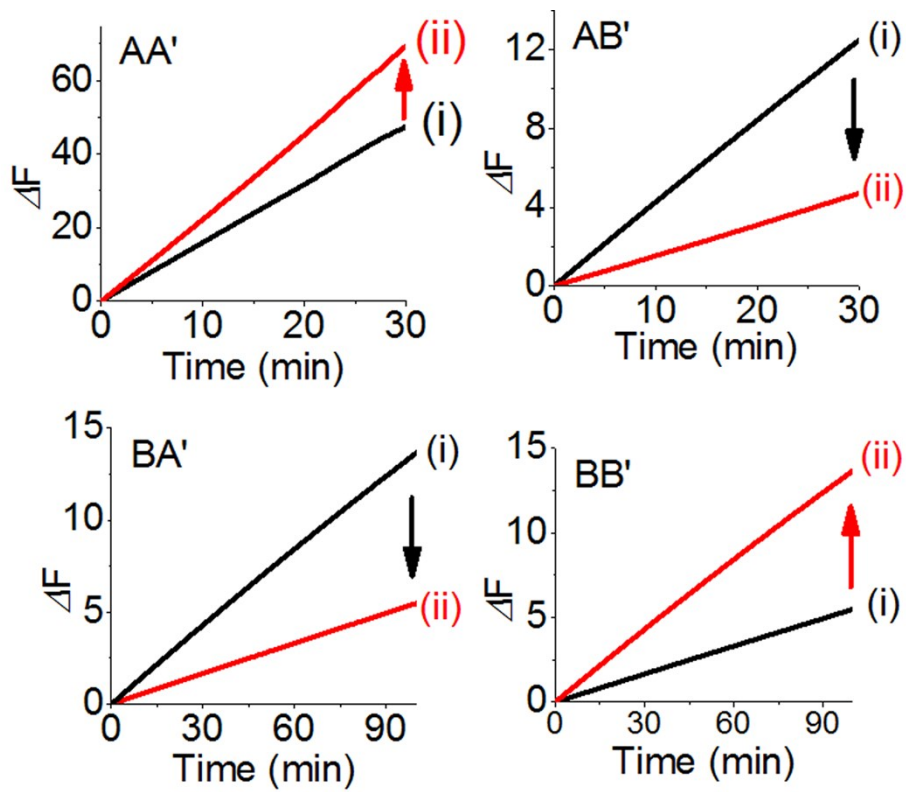


**Figure S29.** Time-dependent fluorescence changes generated by the reporter units associated with the constituents of CDN “X”: Before subjecting to inputs  $I_1$  (i) and after treatment with input  $I_1$  (ii).